Journal of Alloys and Compounds 509 (2011) 9246–9248

Contents lists available at ScienceDirect

Journal of Alloys and Compounds

journal homepage: www.elsevier.com/locate/jallcom

Effect of tunneling barrier as spacer on exchange coupling of CoFeB/AlO_x/Co trilayer structures

Yuan-Tsung Chen*, J.W. Wu

Department of Materials Science and Engineering, I-Shou University, Kaohsiung 840, Taiwan, ROC

ARTICLE INFO

Article history:
Received 4 June 2011
Received in revised form 5 July 2011
Accepted 5 July 2011
Available online 12 July 2011

PACS:
75. 30. Et
75. 60. Nt
75. 70.−i

Keywords:
Magnetic tunnel junctions (MTJs)
Exchange coupling strength
Spacer

ABSTRACT

Magnetic tunneling junctions (MTJs) have a sandwiched structure, which comprises a top ferromagnetic (FM1) layer, an insulating tunneling layer (spacer), and a bottom ferromagnetic (FM2) layer. Exchange coupling in MTJs has been extensively widely examined because the effect of spacer thickness on the ferromagnetic spin-coupling can be exploited in read-head sensors, spin-valve structures, and magntoresistance random access memories (MRAMs). In this investigation, MTJs were deposited in the sequence, glass/CoFeB(50 Å)/AlO_x(d)/Co(100 Å), where the thickness of the AlO_x layer d = 12, 17, 22, 26 or 30 Å. Saturation magnetization (M_s) results demonstrate that the exchange coupling strength and coercivity (H_c) can be varied considerably by varying the tunneling barrier AlO_x spacer. The X-ray diffraction patterns (XRD) include a main peak from hexagonal close-packed (HCP) Co with a highly (0 0 2) textured structure at $2\theta = 44.7^\circ$, and AlO_x and CoFeB are amorphous phases. The full width at half maximum (FWHM) of the Co (0 0 2) peak declines as the AlO_x thickness increases, revealing that the Co layer becomes more crystalline. The magnetic results reveal that the magnetic characteristics are related to the Co crystallinity. The exchange coupling strength increases with AlO_x thickness. The coercivity (H_c) also increases, because the Co crystallinity is eliminated.

1. Introduction

In recent years, increasing attention has been paid to ferromagnetic exchange coupling in magnetic fields [1–3], and the discovery of spintronics has led to a rapid increase in the number of exchange coupling issues of interest. A magnetic tunneling junction (MTJ) has a trilayer structure that is composed of a top ferromagnetic (FM1) layer, an insulating tunneling layer (spacer), and a bottom ferromagnetic (FM2) layer, which can be used in high-density read/write heads, magntoresistance random access memories (MRAM), and gauge sensor fields since spin-dependent tunneling induces a very large magntoresistance [4–10]. The magntoresistance depends on such factors as the indirect spin exchange-coupling of ferromagnetic layers, and the quality of the insulating tunneling layer, which both significantly influence the magnetic performance. However, the fabrication of high-quality junctions requires a ferromagnetic layer with a high spin polarization, perfect microstructure, and proper sufficiently indirect spin exchange-coupling between the FM1 and FM2 layers [11–13]. Chen et al. investigated the Si/Ta/CoFeB/AlO_x/Co/IrMn/Ta and glass/Co/AlO_x/CoFeB systems [14,15]. The results showed that the higher 63% of tunneling magntoresistance (TMR) ratio was obtained in Si/Ta/CoFeB/AlO_x/Co/IrMn/Ta system, and 12% of TMR was obtained in glass/Co/AlO_x/CoFeB system. However, in this glass/CoFeB/AlO_x/Co MTJ, we found a much lower TMR ratio. In short, the higher TMR ratio of MTJ is related to deposited film sequence and different substrate effect. Nevertheless, few investigations of the properties of CoFeB/AlO_x/Co MTJs have been carried out. It is worthwhile to study the tunneling barrier AlO_x as spacer in the magnetic performance. This study focuses on the correlation between the ferromagnetic crystallinity and the magnetic properties. The results demonstrate that a stronger Co (0 0 2) texture is associated with stronger saturation magnetization (M_s) and lower coercivity (H_c).

2. Experimental details

A multilayered MTJ was deposited onto a glass substrate by dc and rf magnetron sputtering system. The typical base chamber pressure was less than 5×10^{-7} Torr, and the Ar working chamber pressure was 5×10^{-3} Torr. The MTJ herein had the structure glass/CoFeB(50 Å)/AlO_x(d)/Co(100 Å) with d = 12, 17, 22, 26 or 30 Å. The target composition of the CoFeB alloy is 40 wt.% Co, 40 wt.% Fe, and 20 wt.% B. To form an AlO_x barrier, Al was firstly deposited on the bottom FM electrode (the CoFeB layer), and the AlO_x layer was then formed by reactive sputtering in an oxidizing atmosphere that was composed of a mixture of Ar/O_2 in the ratio 9:16. The plasma oxidation time varied from 30 to 70 s as the initial thickness of the Al layer increased from 12 Å to 30 Å. To investigate the microstructure, the degree of Co (0 0 2) layer texturing was characterized by X-ray diffraction (XRD) using Cu Kα_1 radiation. The magnetic properties of MTJ were determined using a superconducting quantum interference device (SQUID).

* Corresponding author. Tel.: +886 7657 7711; fax: +886 7657 8444.
E-mail address: ytchen@isu.edu.tw (Y.-T. Chen).

0925-8388/$ – see front matter.
doi:10.1016/j.jallcom.2011.07.007

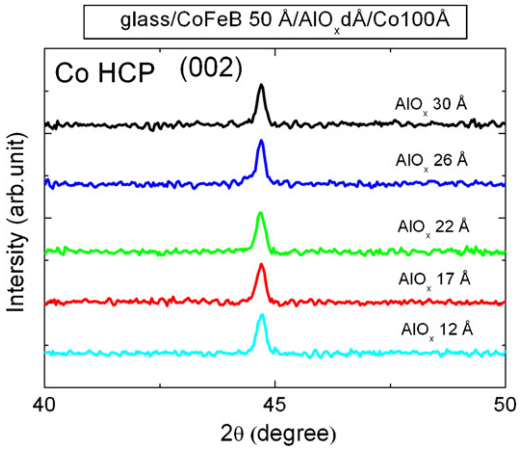

Fig. 1. X-ray diffraction plots of CoFeB(50 Å)/AlO$_x$(dÅ)/Co(100 Å) MTJ.

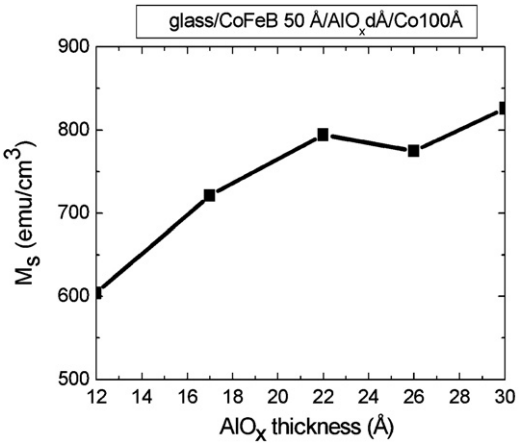

Fig. 3. Dependence of saturation magnetization (M_s) on AlO$_x$ thickness (d) in glass/CoFeB(50 Å)/AlO$_x$(dÅ)/Co(100 Å) junction.

3. Results and discussion

Fig. 1 displays the XRD patterns of the laminated CoFeB(50 Å)/AlO$_x$(d)/Co(100 Å) MTJ junctions. This result demonstrates that the junctions have a hexagonal close-packed (HCP) Co (0 0 2) texture at $2\theta = 44.7^\circ$. Additionally, the microstructures of CoFeB and AlO$_x$ are amorphous. In order to confirm the HCP Co (0 0 2) structure, the Bragg's law can be estimated for d-spacing distance of each diffraction plane [16]. The Bragg's formula can be written as:

$$\lambda = 2d_{hkl} \sin\theta \quad (1)$$

where λ denotes the wavelength of the CuKα$_1$ line; d_{hkl} means the inter-spacing distance of each diffraction plane; and θ is the half angle of the diffraction peak. According to formula (1) calculation, the d_{hkl} of Co is 2.0257 Å. Comparing to previous investigation [17,18], the d_{hkl} of FCC Co (1 1 1) is 2.0467 Å, and the d_{hkl} of hexagonal close-packed Co (0 0 2) is 2.023 Å. It indicates that the HCP Co (0 0 2) exists in this study. We can confirm that the Co structure is hexagonal close-packed. Fig. 2 presents the corresponding full width at half maximum (FWHM, B) of the Co (0 0 2) peak.

Fig. 2 plots the B (FWHM) of the CoFeB(50 Å)/AlO$_x$(d)/Co(100 Å) MTJs as a function of d. Scherrer's formula can be written as,

$$D = 0.9\lambda / B\cos\theta \quad (2)$$

where D is the grain size; λ denotes the wavelength of the CuKα$_1$ line; B is the full width at half maximum of the (0 0 2) peak, and θ is the half angle of the diffraction peak. This formula can be utilized to calculate the grain size and determine the crystallinity [16,19]. As presented in Fig. 2, B is reduced by increasing the AlO$_x$ tunnel barrier thickness, such that the FWHM of the Co layer decreases. This phenomenon explains the increase in the grain size of Co and the enhancement of the Co (0 0 2) texture.

Figs. 3 and 4 present the magnetic properties of CoFeB/AlO$_x$/Co MTJ. First, Fig. 3 plots the saturation magnetization as a function of AlO$_x$ thickness. The M_s of Fig. 3 represents the total spin exchange-coupling contribution of CoFeB/AlO$_x$/Co. Evidently, in our experimental result, in the absence of a spacer tunneling barrier AlO$_x$ layer, the direct spin exchange-coupling effect of the CoFeB/Co bilayer structure is stronger than the indirect spin exchange-coupling effect of the CoFeB/AlO$_x$/Co MTJ, suggesting that inserting a tunneling barrier AlO$_x$ into the CoFeB interface causes an indirect spin exchange-coupling oscillation. The M_s of CoFeB/AlO$_x$/Co MTJ is increased to 850 emu/cm^3 with the AlO$_x$ thickness. Co texturing is therefore reasonably concluded to induce an indirect ferromagnetic spin exchange-coupling interaction between the CoFeB and Co layers. The Co texture of MTJ can be possible concluded that the magneto crystalline anisotropy demonstrates the CoFeB/AlO$_x$/Co exchange-coupling effect, results in higher M_s. Based on this reason, the stronger Co (0 0 2) texture can enhance higher indirect ferromagnetic spin exchange-coupling, revealing the results in Fig. 3.

Fig. 4 plots the dependence of coercivity on the AlO$_x$ thickness (d). From the hysteresis loop result, it exhibits the two-step

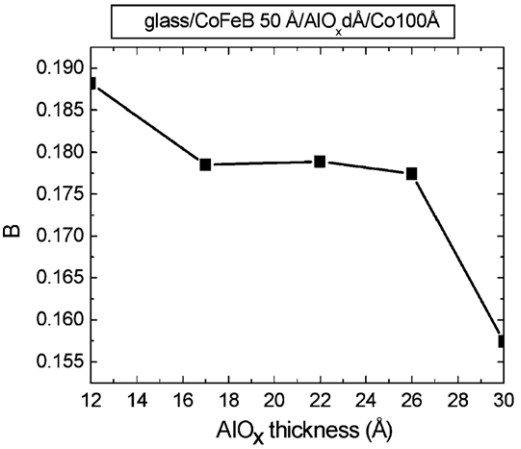

Fig. 2. FWHM (B) as a function of thickness (d) of AlO$_x$ layer.

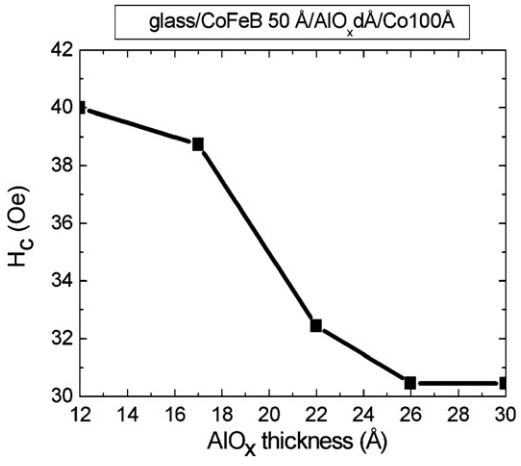

Fig. 4. Coercivity (H_c) as a function of AlO$_x$ thickness (d) in glass/CoFeB(50 Å)/AlO$_x$(dÅ)/Co(100 Å) junction.

characteristic, we can infer the anti-parallel alignment between the CoFeB and Co layers. When the external field (H) switches the CoFeB/AlO_x/Co, it initially rotates the coercivity of CoFeB, then as a larger field H, the coercivity of Co is rotated to saturation. H_c falls as the AlO_x thickness increases. A possible cause is the spin coupling and the degree of decoupling of CoFeB/AlO_x/Co in this situation. The Co (0 0 2) texture can strengthen the spin exchange-coupling arrangement. From Fig. 2, a thinner AlO_x is associated with a larger FWHM, and a weaker Co (0 0 2) texture. When the external field (H) is used to switch the MTJ junction, it must rotate the CoFeB and Co layers, increasing the H_c value. In contrast, the Co (0 0 2) texture can strengthen the spin exchange-coupling interaction between the CoFeB and Co layers as the AlO_x layer becomes thicker. The rotated field (H) only switches the CoFeB/AlO_x/Co exchange-coupling field, reducing the H_c value. From the magneto crystalline anisotropy, the stronger Co (0 0 2) texture induces the higher indirect CoFeB/AlO_x/Co exchange-coupling interaction. The weaken Co (0 0 2) texture reduces the lower CoFeB/AlO_x/Co exchange-coupling interaction. When the external field (H) rotates the weaken Co (0 0 2) texture of CoFeB/AlO_x/Co MTJ, it must rotate the coercivity of CoFeB and Co layers individually, results in higher H_c value. Another possible cause may be the polarization and depolarization of spin tunneling in the oxidation plasma process. Briefly, if d is thin (for example, d = 12 Å), then the CoFeB bottom electrode may become over-oxidized, causing the oxidation at the CoFeB/AlO_x interface. The surface pinning effect at the CoFeB/AlO_x interface may produce some defects, such as inclusions, and may result in oxidation and roughness. The defects can make motion of the domain walls difficult and increase H_c [20].

4. Conclusions

CoFeB(50 Å)/AlO_x(dÅ)/Co(100 Å) MTJs were fabricated to examine their microstructure and magnetic properties, including M_s and H_c, as functions of the AlO_x barrier thickness d (which was varied from 12 to 30 Å). The microstructure of the MTJs reveals that the Co (0 0 2) texture becomes stronger as the thickness of the AlO_x layer increases. The FWHM of the Co (0 0 2) texture falls as the thickness of the tunneling barrier AlO_x is increased. This phenomenon explains why the grain size of Co increases and the Co (0 0 2) texture becomes stronger. Furthermore, the relationship between the Co (0 0 2) texture and the magnetic properties suggests that the enhanced Co (0 0 2) texture increases the saturation magnetization and reduces the coercivity. Higher H_c values are obtained at thinner AlO_x thicknesses, because the spin decoupling effect occurs between the CoFeB and Co layers and because of the domain pinning over the oxidized CoFeB/AlO_x interface.

Acknowledgements

This work was supported by the National Science Council and I-Shou University, under grants nos. NSC100-2112-M-214-001-MY3 and ISU98-S-02, respectively. The authors would like to thank Professor S. U. Jen for his assistance and NSC instrument of NSYSU for SQUID measurement.

References

[1] F. Hoffmann, A. Stankoff, H. Pascard, J. Appl. Phys. 41 (2009) 1022.
[2] D. Mauri, H.C. Siegmann, P.S. Bagus, E. Kay, J. Appl. Phys 62 (1987) 3047.
[3] Ken-ichi Imakita, Masakiyo Tsunoda, Migaku Takahashi, Appl. Phys. Lett. 85 (2004) 3812.
[4] Y.T. Chen, S.U. Jen, Y.D. Yao, J.M. Wu, A.C. Sun, Appl. Phys. Lett. 88 (2006) 222509.
[5] J.R. Childress, M.J. Carey, S. Maat, N. Smith, R.E. Fontana, D. Druist, K. Carey, J.A. Katine, N. Robertson, T.D. Boone, M. Alex, J. Moore, C.H. Tsang, IEEE Trans. Magn 44 (2008) 90.
[6] S.S.P. Parkin, N. More, K.P. Roche, Phys. Rev. Lett. 64 (1990) 2304.
[7] T. Moriyama, C. Ni, W.G. Wang, X. Zhang, J.Q. Xiao, Appl. Phys. Lett. 88 (2006) 222503.
[8] Y.T. Chen, S.U. Jen, Y.D. Yao, J.M. Wu, C.C. Lee, A.C. Sun, IEEE Trans. Magn. 42 (2006) 278.
[9] David D. Djayaprawira, Koji Tsunekawa, Motonobu Nagai, Hiroki Maehara, Shinji Yamagata1, Naoki Watanabe, Shinji Yuasa, Yoshishige Suzuki, Koji Ando, Appl. Phys. Lett. 86 (2005) 092502.
[10] J. Hayakawa, S. Ikeda, Y.M. Lee, F. Matsukura, H. Ohno, Appl. Phys. Lett. 89 (2006) 232510.
[11] Y.T. Chen, J.Y. Tseng, C.C. Chang, W.C. Liu, Jason S.C. Jang, J. Alloys Compd. 489 (2010) 242.
[12] N.P. Aley, G. Vallejo-Fernandez, R. Kroeger, B. Lafferty, J. Agnew, Y. Lu, K. O'Grady, IEEE Trans. Magn. 44 (2008) 2820.
[13] G. Anderson, Y. Huai, L. Milowslawsky, J. Appl. Phys. 87 (2000) 6989.
[14] Y.T. Chen, S.U. Jen, T.L. Tsai, C.Y. Huang, Y.D. Yao, J. Appl. Phys. 103 (2008) 07A901.
[15] Y.T. Chen, J.Y. Tseng, S.R. Jian, H.G. Chen, S.U. Jen, J. Alloys Compd. 485 (2009) 822.
[16] B.D. Cullity, Elements of X-ray Diffraction , 2nd ed., Addison-Wesley, Reading, MA, 1978.
[17] J.J. Yang, G.X. Ji, Y. Yang, H. Xiang, Y.A. Chang, J. Electron. Mater. 37 (2008) 355.
[18] A. Kharmouche, S.M. Chérif, A. Bourzami, A. Layadi, G. Schmerber, J. Phys. D: Appl. Phys. 37 (2004) 2583.
[19] Y.T. Chen, C.C. Chang, J. Alloys Compd. 498 (2010) 113.
[20] Y.T. Chen, Y.C. Lin, S.U. Jen, J.Y. Tseng, Y.D. Yao, J. Alloys Compd. 509 (2011) 5587.